Bioresource Technology 359 (2022) 127466

Contents lists available at ScienceDirect

Bioresource Technology

journal homepage: www.elsevier.com/locate/biortech

Valorization of hydrolysis lignin from a spruce-based biorefinery by applying γ-valerolactone treatment

Forough Momayez [a], Mattias Hedenström [a], Stefan Stagge [a], Leif J. Jönsson [a], Carlos Martín [a,b,*]

[a] Umeå University, Department of Chemistry, SE-901 87 Umeå, Sweden
[b] Inland Norway University of Applied Sciences, Department of Biotechnology, N-2317 Hamar, Norway

HIGHLIGHTS

- Hydrolysis lignin was treated with γ-valerolactone (GVL)
- The effect of temperature, LSR and sulfuric acid on lignin extraction was assessed.
- Assisting the treatment with sulfuric acid favored lignin solubilization in GVL.
- Extracted lignin was regenerated by small additions of water to treatment liquors.
- Lignins from acid-assisted GVL treatment had broad molecular weight distribution.

GRAPHICAL ABSTRACT

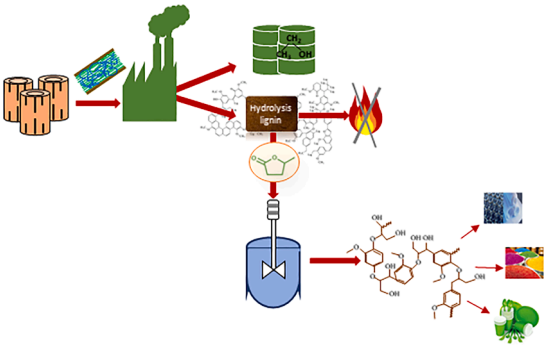

ARTICLE INFO

Keywords:
Hydrolysis lignin
γ-valerolactone
Biorefinery
Lignocellulose
Enzymatic saccharification

ABSTRACT

Hydrolysis lignin, i.e., the hydrolysis residue of cellulosic ethanol plants, was extracted with the green solvent γ-valerolactone (GVL). Treatments at 170–210 °C were performed with either non-acidified GVL/water mixtures (NA-GVL) or with mixtures containing sulfuric acid (SA-GVL). SA-GVL treatment at 210 °C resulted in the highest lignin solubilization (64% (w/w) of initial content), and 76% of the solubilized mass was regenerated by water-induced precipitation. Regenerated lignins were characterized through compositional analysis with sulfuric acid, as well as using pyrolysis–gas chromatography/mass spectrometry (Py-GC/MS), high-performance size-exclusion chromatography (HPSEC), solid-state cross-polarization/magic angle spinning ^{13}C nuclear magnetic resonance (CP/MAS ^{13}C NMR) spectroscopy, ^{1}H–^{13}C heteronuclear single-quantum coherence NMR (HSQC NMR), and Fourier-transform infrared (FTIR) spectroscopy. The characterization revealed that the main difference between regenerated lignins was their molecular weight. Molecular weight averages increased with treatment temperature, and they were higher and had broader distribution for SA-GVL lignins than for NA-GVL lignins.

1. Introduction

The use of fossil fuels for satisfying the energy demand causes sustainability problems associated with greenhouse gas emissions. Therefore, other energy platforms, including wind, water, solar fuels, and biomass, attract a great deal of attention (Ashokkumar et al., 2022;

* Corresponding author at: Inland Norway University of Applied Sciences, Department of Biotechnology, N-2317 Hamar, Norway.
E-mail address: carlos.medina@inn.no (C. Martín).

https://doi.org/10.1016/j.biortech.2022.127466
Received 30 April 2022; Received in revised form 8 June 2022; Accepted 10 June 2022
Available online 13 June 2022

Lowe and Drummond, 2022). Lignocellulosic biomass, which is composed of cellulose, hemicelluloses and lignin, is an abundant renewable carbon source, and it can be processed in biorefineries for producing biofuels and other bio-based products (Martín et al., 2022) and thus contribute to a portion of the demand for renewable energy. Around 182 billion tons of lignocellulosic biomass are produced annually worldwide (Ashokkumar et al., 2022). Lignocellulose can be used through the sugar-platform route, which is based on enzymatic saccharification of cellulose, microbial fermentation or chemical conversion of the resulting sugars, and valorization of the residual lignin (Galbe and Wallberg, 2019; Martín et al., 2022). Enzymatic saccharification of cellulose is affected by lignin and hemicelluloses and by other factors contributing to feedstock recalcitrance. A pretreatment step is typically implemented to facilitate enzymatic saccharification (Galbe and Wallberg, 2019; Martín et al., 2022).

Despite the efforts to develop efficient pretreatment methods and versatile enzyme preparations, effective lignocellulose bioconversion is challenged by several problems. For instance, cellulose saccharification typically results in incomplete conversion, and a cellulose portion remains in the solid residue together with lignin. The enzymatic hydrolysis residue, hereafter referred to as hydrolysis lignin (HL), is composed of lignin and non-hydrolyzed cellulose with minor fractions of hemicelluloses, extractives and ash, depending on pretreatment and saccharification efficiency and on the used raw material (Xu et al., 2021).

Lignin is an aromatic polymer primarily composed of three phenylpropane units, namely syringyl (S), guaiacyl (G), and *p*-hydroxyphenyl (H). They are mainly connected via ether and carbon–carbon bonds (Ralph et al., 2019). Technical lignins include kraft lignin (from kraft pulping), lignosulfonates (from sulfite pulping), HL (from biochemical conversion), and lignins from non-conventional pulping methods.

Ethanol is the most widespread lignocellulose-based biofuel that is commercially available (Singh et al., 2022). A current challenge is how to use the large amounts of HL remaining after enzymatic saccharification. HL is mainly used as energy carrier at cellulosic ethanol plants, but since 60% of the generated amounts would be enough to meet the energy requirements of the plants, a large surplus is available (Ragauskas et al., 2014). Processing of one ton of softwood to ethanol results in around 350–400 kg of HL as average (Evstigneyev et al., 2016). Based on the global production data, and assuming 355 L bioethanol per ton of dry biomass (Ragauskas et al., 2014), approximately 281 million tons of biomass are required annually, and that generates around 108 million tons of HL. Finding high-added value applications for HL would make cellulosic ethanol production, and lignocellulose biorefining in general, more profitable. High lignin purity is required for high-added value applications, but technical lignins, including HL, are qualitatively different from preparations of pure lignin. Furthermore, the relatively high cellulose content of HL might be an impediment for some applications. Therefore, lignin separation from other HL components without causing further transformations is an important first step for its valorization. That can be implemented by selective extraction of lignin with an appropriate solvent system.

γ-Valerolactone (GVL) is a biomass-derived polar aprotic solvent, which has recently attracted interest for biomass pretreatment (Jia et al., 2020), and for lignin fractionation (Wang et al., 2019), but it has not yet been directly applied to HL. GVL has high thermal and chemical stability, and it is non-toxic, non-flammable, and non-volatile (Alonso et al., 2013). Furthermore, it has high boiling point, and is miscible with water without forming an azeotrope, which facilitates recycling by simple distillation (Yin et al., 2021). The application of GVL/water mixtures for biomass fractionation is an approach of high interest considering that GVL is effective towards lignin solubilization, while water is necessary for hydrolysis of hemicelluloses (Jia et al., 2020; Lê et al., 2016). Although GLV mixtures with other solvents, e.g., DMSO and DMF, can also be used, high lignin solubilization has been reported for GVL/water mixtures (Xue et al., 2016). Another positive issue is that in presence of GVL the activation energy of hydrolysis of glycosidic bonds decreases, while further reactions of formed sugars are not affected. Hence, minimal sugar degradation is expected when running biorefinery operations in GVL/water solvent systems (Shuai et al., 2016).

Considering the solubility of lignin in GVL, using GVL/water solvent systems is a potential approach for HL valorization. The current work was aimed at evaluating the use of GVL/water mixtures for selective extraction of lignin from the HL matrix, using softwood HL produced under industrial-like conditions as starting material. The effects of treatment temperature, liquid-to-solid ratio, and H_2SO_4 addition on lignin solubilization were assessed. The solubilized lignin was precipitated by water addition, and characterized using advanced analytical techniques, e.g., compositional analysis, pyrolysis–gas chromatography/mass spectroscopy, high-performance size-exclusion chromatography, cross polarization/magic-angle spinning nuclear magnetic resonance, Fourier-transform infrared spectroscopy, and heteronuclear single-quantum coherence nuclear magnetic resonance spectroscopy.

2. Material and methods

2.1. Materials

HL from the Biorefinery Demonstration Plant, Örnsköldsvik, Sweden, was provided by SEKAB (https://www.sekab.com/en/). It was the solid residue from the enzymatic saccharification of pretreated Norway spruce (*Picea abies*) sawdust. Pretreatment was performed by SEKAB E-Technology AB by impregnating sawdust with SO_2, heating it with steam and holding it at 200 °C for 15 min. Further pretreatment details were reported previously (Oliva-Taravilla et al., 2020). Enzymatic saccharification was conducted with a 20% (w/w) total solids load at 50 °C and for 72 h using a state-of-the-art preparation of cellulolytic enzymes from a leading enzyme manufacturer. The hydrolysate was separated using a filter press, and the solid fraction (HL) was washed with water. The washed HL was air-dried at room temperature until it reached a dry matter content above 90% (w/w). Then it was milled using an A11 basic analytical mill (IKA-Werke GmbH, Staufen, Germany). The moisture content of the HL was determined using an HG63 moisture analyzer (Mettler-Toledo, Greifensee, Switzerland). All the used chemicals were purchased from Sigma-Aldrich (Steinheim, Germany).

2.2. GVL treatment of HL

HL was treated with GVL mixed with either water or dilute sulfuric acid. In the treatment with non-acidified GVL (NA-GVL), 80:20 GVL/water mixtures were added to HL at liquid-to-solid ratios (LSR) of 7, 10, and 20 (v/w). Treatments were conducted in a 1-L Parr reactor (Parr Instrument, Moline, IL, USA). HL was suspended in 270 mL of the GVL/water mixture, and the suspension was heated to either 170, 190, or 210 °C, and held for 2 h. In the sulfuric acid-assisted GVL treatment (SA-GVL), HL was mixed with 270 mL of 80:20 GVL/water solution at LSR 10. Sulfuric acid was added to a concentration of 5 mM, and treatments were run at either 170, 190, or 210 °C for 1 h. At the end of treatments, the system was cooled with cold water through an internal coil, and the slurry was vacuum-filtered. The solid phase was washed with 500 mL of distilled water, and air-dried at room temperature. The liquid phase, i.e., treatment liquor, was stored at 5 °C until further experiments.

2.3. Lignin precipitation

The solubilized lignin was precipitated from the treatment liquor by adding a two-fold volume of deionized water as antisolvent. After water addition, the mixture was left overnight at 5 °C for precipitation. The suspension was centrifuged using an Avanti J-26 XP centrifuge (Beckman, Palo Alto, CA, USA) at 8500 rpm for 30 min. After removing the supernatant, the precipitate was washed twice with portions of 200 mL

of warm (40 °C) deionized water with stirring (750 rpm) for 2 h. The precipitated lignin, hereafter referred to as regenerated lignin, was collected by vacuum filtration, and it was air-dried for further characterization.

2.4. Compositional analysis of treated HL

Two-step treatment with sulfuric acid (TSSA), performed mainly according to the NREL/TP-510–42618 protocol (Sluiter et al., 2008), was applied to HL, treatment residues, and regenerated lignins for determining the content of lignin and structural carbohydrates. Acid-insoluble (Klason) lignin was determined gravimetrically as the TSSA solid residue, while acid-soluble lignin was determined spectrophotometrically. The concentration of monosaccharides was analyzed by high-performance anion-exchange chromatography (HPAEC), and the values were used for calculating the content of polysaccharides according to previously reported methodology (Ilanidis et al., 2021b). HPAEC was performed with an ICS-5000 system (Dionex, Sunnyvale, CA, USA) equipped with a CarboPac PA1 (4 × 250 mm) column and with a CarboPac PA1 (4 × 50 mm) guard column (all from Dionex). Before analysis, the samples were diluted with ultrapure water and then filtered through 0.20 μm nylon membranes in syringe-driven filters. Ultrapure water was used as mobile phase at an elution rate of 1 mL/min. The column was regenerated prior to injection by a solution containing 60% of 300 mM sodium hydroxide and 40% of a mixture of 200 mM sodium hydroxide and 170 mM sodium acetate. After that, ultrapure water was applied for 3 min to equilibrate the column. Pulsed amperometric detection with a gold working electrode and Ag/AgCl as reference electrode was used. To amplify the signals, post column addition of sodium hydroxide solution (300 mM) with a flow rate of 0.5 mL/min was applied. The Chromeleon 7.1 software (Dionex) was utilized to calculate the concentration of monosaccharides. The experiments were conducted in triplicate and the mean values are reported. The statistical significance of the differences between the mean values was determined by using the GLM (Generalized Linear Model) method and the SAS 9.4 software (SAS Institute Inc., Cary, NC, USA).

2.5. Analysis of the treatment liquor

Monosaccharides were determined by HPAEC as described in section 2.4. Furfural and 5-hydroxymethylfurfural (HMF) were determined by high-performance liquid chromatography (HPLC) using an Agilent Infinity 1260 system (Agilent, Santa Clara, CA, USA) equipped with a diode-array detector and a 3 × 50 mm, 1.8 μm Zorbax RRHT SB-C18 column. An aqueous solution of 0.1% (v/v) formic acid and 3% (v/v) acetonitrile with the rate of 0.5 mL/min was used as mobile phase. The column temperature was set to 40 °C. The experiments were conducted in triplicate and the mean values are reported. The analyses were performed in triplicate, and the statistical processing of the mean values was performed as described in section 2.4.

2.6. Pyrolysis-gas chromatography/mass spectrometry (Py-GC/MS) analysis

Py-GC/MS analysis, based on the method described by Gerber et al. (2012), was applied to achieve additional information on the content of lignin and carbohydrates in HL, treatment residues and regenerated lignins. The content of pseudo-lignin was estimated as:

$$\Delta_{Lignin} = [(K_L + A_{SL}) - P_L] \quad (1)$$

Where Δ_{Lignin} is pseudo-lignin (%), K_L and A_{SL} are the mass fractions (%) of Klason lignin and acid-soluble lignin, respectively, obtained from TSSA compositional analysis, and P_L is the peak area fraction (%) assigned to lignin in the Py-GC/MS analysis.

2.7. High-Performance size exclusion chromatography (HPSEC)

The molecular weight distributions of regenerated lignins were determined by using high-performance size exclusion chromatography (HPSEC). The system consisted of a Polymer Laboratories PL-GPC 50 Plus instrument (Agilent, Santa Clara, CA, USA) coupled to a Multi-Angle Light Scattering (MALS) detector. DMSO was used as solvent. The HPSEC system was equipped with a guard column and two serial T6000M columns from Malvern. The temperatures were set at 50 °C, and the flow rate was 0.5 mL min^{-1}. The detection system consisted of a refractive index (RI) detector and a multi-angle laser light scattering (MALS) detector. Two pullulan standards (PSS) were used to calibrate the detectors. The data were evaluated by using the OMNISEC V11 software from Malvern.

2.8. Nuclear magnetic resonance (NMR) spectroscopy

Two-dimensional ^{1}H–^{13}C Heteronuclear Single-Quantum Coherence Nuclear Magnetic Resonance (HSQC NMR) spectroscopy was used for characterization of regenerated lignins, while Cross Polarization/Magic-Angle Spinning (CP/MAS) ^{13}C NMR was applied to regenerated lignins, HL and treatment residues. The HSQC NMR spectra were acquired at 25 °C using a Bruker 600 MHz Avance III HD spectrometer, equipped with a 5 mm broadband observe cryoprobe with z-gradients and a SampleJet auto-sampler. Thirty mg of each sample was dissolved in 600 μL DMSO-d_6 and transferred to 5 mm NMR tubes. The spectra were recorded using adiabatic ^{13}C inversion pulses with sweep-widths of 8.14 and 140 ppm in the ^{1}H and ^{13}C dimensions, respectively, and with a relaxation delay of 1.5 s. For each of the 256 increments in the indirect dimension, 20 scans were recorded. Zero filling in the indirect dimension was applied, resulting in 1024 × 512 spectral matrices. A Gaussian window function with a line-broadening of −0.1 Hz for ^{1}H, −1 Hz for ^{13}C, and a Gaussian Broadening of 0.001 in both dimensions was applied prior to the Fourier transformation. Spectra were processed in Topspin 3.6 (Bruker Biospin, Germany). The CP/MAS ^{13}C NMR spectra were obtained on a 500 MHz Advance III spectrometer equipped with a 4 mm MAS probe. Approximately 80 mg of pulverized sample was packed into a 4 mm ZrO_2 rotor. A spin-rate of 10 kHz was used, the contact time was 1 ms, and 4 096 scans were collected for each sample. A Gaussian window function was used in the spectral processing performed in Topspin 3.2 (Bruker Biospin). Samples were analyzed at ambient temperature.

2.9. Fourier-transform infrared (FTIR) spectroscopy

FTIR spectroscopy was applied to study structural features of regenerated lignins, HL, and treatment residues. The samples were first ground with SpectroGrade potassium bromide (Fisher Scientific, Waltham, MA, USA). A Bruker IFS 66v/S FTIR spectrometer with a standard Deuterated Triglycine Sulfate detector, and fitted with a diffuse reflectance accessory (Bruker Corporation, Billerica, MA, USA), was used for recording the spectra. Baseline correction and vector normalization over the entire spectral region was done with OPUS software (version 7, Bruker Optik GmbH, Ettlingen, Germany).

3. Results and discussion

3.1. Effects of treatment conditions on lignin solubilization and on composition of solid residues

The compositional analysis revealed that HL contained 53.5% (w/w) total lignin, 42.9% (w/w) glucan, and 3.5% (w/w) hemicelluloses (Table 1). The main hemicellulosic components were (in % (w/w)) mannan (1.7), xylan (1.1), and galactan (0.7) (data not shown). Although one might expect higher lignin content, the observed value is consistent with previous reports. For instance, the residue of enzymatic

Table 1
Yield and composition of treated solids and fraction of solubilized lignin after NA-GVL treatment (non-acidified GVL/water mixture treatment for 120 min) and SA-GVL treatment (sulfuric acid-assisted GVL/water mixture treatment for 60 min). Means of triplicate analyses. Different superscripted uppercase letters denote significant differences at an alpha level of 0.05 according to a Fisher's least significant difference (LSD) test. Like-lettered groups are not significantly different.

Treatment	Temperature (°C)/ LSR[a]	Yield of treated solids, % (w/w)	Composition of treated solids, % (w/w)			Solubilized lignin, % (w/w)	Recovered glucan in treated solid residues % (w/w)
			Glucan	Total lignin	Hemicelluloses		
Non-treated hydrolysis lignin			42.9^{D} (1.9)	53.5^{A} (1.2)	3.5 (1.0)	–	–
NA-GVL	170/7	83	45.3^{CD} (1.8)	44.7^{CDE} (<0.1)	ND[b]	31.3	87.6
NA-GVL	170/10	84	46.3^{BCD} (1.7)	45.3^{C} (0.3)	ND	29.5	90.7
NA-GVL	170/20	83	46.5^{BCD} (1.4)	45.2^{CD} (1.2)	ND	30.5	90.0
NA-GVL	190/7	83	45.7^{BCD} (1.6)	44.1^{E} (2.2)	ND	32.2	88.4
NA-GVL	190/10	79	47.4^{BCD} (1.6)	44.2^{DE} (0.4)	ND	35.3	87.3
NA-GVL	190/20	74	50.3^{AB} (2.5)	43.9^{E} (0.3)	ND	39.8	86.8
NA-GVL	210/7	74	46.8^{BCD} (5.6)	41.6^{F} (0.5)	ND	43.0	80.7
NA-GVL	210/10	73	48.9^{BC} (0.9)	40.0^{G} (0.5)	ND	45.9	83.2
NA-GVL	210/20	70	50.4^{AB} (5.9)	39.6^{G} (0.8)	ND	52.6	82.2
SA-GVL	170/10	81	49.1^{BC} (2.1)	46.3^{B} (1.0)	ND	30.6	92.7
SA-GVL	190/10	70	54.6^{A} (2.9)	41.1^{F} (0.1)	ND	46.7	89.1
SA-GVL	210/10	35	49.6^{BC} (2.2)	39.3^{G} (1.0)	ND	63.9	40.5

[a] LSR, liquid-to-solid ratio. Numbers in parentheses show standard deviations.
[b] ND: Not detected.

hydrolysis of spruce pretreated by SO_2-assisted steam-explosion at 215 °C for 5 min had 52.8% lignin content (Várnai et al., 2010). Depending on substrate composition and pretreatment and hydrolysis conditions, lignin content of HL varies within a wide range. The residue of enzymatic hydrolysis of corn straw pretreated by steam explosion at 1.5 MPa for 5 min contained 60 % (w/w) lignin (Liu et al., 2018), while HL of eucalyptus chips pretreated with hot water for 20 min at 170 °C followed by enzymatic hydrolysis contained 62% lignin, and it increased to 90% by increasing pretreatment temperature and applying wet disk milling (Weiqi et al., 2013).

For the NA-GVL experiments, lignin solubilization around 30% (w/w) of the initial content was achieved after treatments at 170 °C, 32 – 40% at 190 °C, and 43 – 53% at 210 °C (Table 1). No effect of the LSR on lignin solubilization was observed during treatment at 170 °C, whereas at 190 and 210 °C, solubilization increased with LSR increase. The yield of residual solids after treatment was generally high, especially in the experiments at 170 °C. Lignin content in treated solids decreased from 53.5% in HL to 44 – 45% in the residual solids of treatments at 170 and 190 °C, and to around 40% or below in those of treatments at 210 °C. Glucan content increased from 42.9% in HL to 45 – 50% in the treatment solids. Glucan recovery in the treated solids was 87 – 91% for treatments at 170 and 190 °C, and 80 – 83% for treatments at 210 °C, while hemicelluloses were completely solubilized in all experimental conditions. In NA-GVL treatments, the lowest yield of residual solids (70% (w/w)) and the lowest lignin content (39.3%) were observed for the material treated at 210 °C and LSR 20. It was evident that increasing temperature from 190 °C to 210 °C was much more effective for lignin solubilization than increasing it from 170 °C to 190 °C.

The SA-GVL treatments were performed for a shorter period of time than the NA-GVL treatments, with the intention to avoid major lignin degradation by long exposure to an acidic environment. In SA-GVL treatments, only one LSR was evaluated, as no effect of LSR on solubilization was observed in pilot trials. For SA-GVL treatment at 170 °C, lignin solubilization was 30.6% (w/w) (Table 1), which is comparable with the NA-GVL treatment at similar temperature. As the temperature increased, a proportional increase of lignin solubilization, more remarkable than that for NA-GVL treatment, was observed. At 210 °C, solubilization of around two thirds of the initial lignin was reached in the SA-GVL treatment. In accordance with the lignin solubilization pattern, the yield of treated solids decreased to 35% (w/w) at 210 °C, and lignin content in the treated solids decreased to 39.3% (w/w). It is noteworthy that despite the major lignin removal by the treatment at 210 °C, the increase of the glucan mass fraction in the treated solids, compared with that of HL, was rather modest, and that glucan recovery was only 40.5% of the initial content (Table 1). The occurrence of cellulose hydrolysis might have been behind that phenomenon, which was less remarkable at lower temperatures, where glucan recovery was around 90%.

3.2. Content of sugars and furan aldehydes in the treatment liquors

In the liquors from NA-GVL treatments, glucose concentrations were always below 0.6 g/L, and they increased only slightly with the increase of the temperature (Table 2). The low glucose formation reveals that cellulose contained in HL was hydrolyzed to very limited extent during the treatment, even for the experiments performed at 210 °C. Mannose concentrations were below 0.3 g/L, and the detected concentrations of xylose and galactose were even lower (data not shown). The concentrations of all hemicellulosic sugars decreased clearly with the increase of treatment temperature. That suggests that hemicelluloses, whose content in HL was low (Table 1), were hydrolyzed already at 170 °C, and the released sugars underwent degradation. Remarkable sugar degradation occurred at high treatment temperature, as can be inferred from the high formation of 5-hydroxymethylfurfural (HMF) and furfural at 190 and 210 °C. The furan aldehydes HMF and furfural are formed by dehydration of, respectively, hexoses and pentoses during thermal treatments under acidic conditions (Jönsson and Martín, 2016). The relatively high sensitivity of hemicelluloses to treatments at high temperature and low pH (between 3.2 and 3.7, Table 2) explains the formation of furan aldehydes. The concentration of HMF in the treatment liquors was higher than that of furfural. That can be explained by the softwood origin of the investigated HL. Softwood hemicelluloses are

Table 2
Concentration (g/L) of sugars and furan aldehydes in the liquors from the treatments. The codification is the same as in Table 1. Means of triplicate analyses. Different superscripted uppercase letters denote significant differences at an alpha level of 0.05 according to a Fisher's least significant difference (LSD) test. Like-lettered groups are not significantly different.

Treatment	Temperature (°C)/LSR	Glucose	Mannose	HMF	Furfural	pH
NA-GVL	170/7	0.38^{EF} (0.01)	0.28^{C} (0.02)	0.71^{E} (0.01)	0.26^{E} (0.01)	3.4
NA-GVL	170/10	0.29^{FG} (0.01)	0.26^{D} (<0.01)	0.42^{FG} (0.01)	0.16^{G} (<0.01)	3.5
NA-GVL	170/20	0.15^{I} (<0.01)	0.17^{FG} (<0.01)	0.18^{H} (<0.01)	0.07^{I} (<0.01)	3.7
NA-GVL	190/7	0.58^{C} (0.01)	0.18^{EF} (<0.01)	1.24^{C} (0.07)	0.33^{D} (0.01)	3.4
NA-GVL	190/10	0.44^{DE} (<0.01)	0.16^{G} (<0.01)	0.77^{E} (0.06)	0.22^{F} (0.02)	3.5
NA-GVL	190/20	0.28^{GH} (0.02)	0.18^{E} (<0.01)	0.35^{G} (0.01)	0.11^{H} (<0.01)	3.6
NA-GVL	210/7	0.48^{D} (0.01)	0.05^{I} (<0.01)	1.92^{B} (0.06)	0.43^{B} (0.06)	3.2
NA-GVL	210/10	0.42^{DE} (0.02)	0.06^{I} (<0.01)	1.28^{C} (0.05)	0.31^{D} (0.05)	3.2
NA-GVL	210/20	0.19^{HI} (<0.01)	0.04^{J} (<0.01)	0.52^{F} (0.01)	0.13^{H} (0.01)	3.2
SA-GVL	170/10	0.63^{C} (0.10)	0.38^{A} (0.01)	0.46^{F} (0.02)	0.20^{F} (0.01)	2.6
SA-GVL	190/10	2.14^{B} (0.07)	0.33^{B} (0.01)	1.06^{D} (0.06)	0.40^{C} (0.02)	2.4
SA-GVL	210/10	6.45^{A} (0.14)	0.14^{H} (<0.01)	3.70^{A} (0.19)	0.94^{A} (0.05)	2.4

predominantly hexosans (Fengel and Wegener, 1989), and, therefore, HMF is the primary dehydration product to be expected. The hydrolysis of hemicelluloses, as elucidated from the composition of the treatment liquors (Table 2), at all treatment temperatures correlates well with their absence in all treated solids (Table 1). By increasing the LSR, the concentrations of sugars and furan aldehydes decreased, which is a dilution effect caused by adding higher volumes of liquid to the initial mass of HL in the reaction mixture.

The glucose concentrations were higher in the liquors from SA-GVL treatments (Table 2) than in those from the treatments with NA-GVL, which might be explained by the occurrence of acid-catalyzed hydrolysis of cellulose. The glucose concentration increased with increasing temperature, and reached 6.45 g/L in the liquor from the treatment at 210 °C. This result matches well with the previously discussed low glucan recovery in treated solids (Table 1). The trend observed for the hemicellulosic sugars was similar to that discussed for NA-GVL treatments. The formation of furan aldehydes in SA-GVL treatments, especially at the highest temperature, was higher than in NA-GVL experiments. At 210 °C, the HMF concentration reached 3.70 g/L in SA-GVL treatments, while it was 1.28 g/L in NA-GVL treatments. The furfural concentration was 0.94 g/L for SA-GVL and 0.31 g/L for NA-GVL. The higher formation of furan aldehydes in SA-GVL is the result of increased acid-catalyzed sugar dehydration. The HMF concentration in the liquor from SA-GVL treatment at 210 °C was higher than what could be expected from the mannan and galactan, as well as hemicellulosic glucan, contained in HL. The high HMF formation can be explained by the degradation of glucose resulting from cellulose hydrolysis.

3.3. Lignin regeneration

Solubilized lignin was regenerated from the treatment liquors by precipitation, which was induced by adding water as antisolvent. Precipitated lignin was then separated from the diluted liquor by centrifugation. Up to 56% (w/w) of the lignin contained in HL was recovered by sulfuric-acid-assisted GVL treatment at 210 °C (Fig. 1). That is equivalent to 74% of the lignin that was solubilized by that treatment. Lower recovery was achieved for treatment with NA-GVL, where the highest yield out of the initial content was around 28%, which corresponds to 67% of the solubilized mass. The solubilized lignin was easier to regenerate not only when sulfuric acid was present in the initial reaction mixture, but it was rather typical for liquors from treatment conditions resulting in higher lignin solubilization. For instance, for NA-GVL treatments, the yield of regenerated lignin out of the solubilized mass was 48 – 67% (w/w) for the experiments at 210 °C (Fig. 1), which had resulted in 43 – 53% solubilization (Table 1), but it was below 40% for experiments at 170 °C, which had resulted in ~ 30% solubilization. It is also noteworthy that for NA-GVL treatments at 190 and 210 °C, the yield of regenerated lignin out of the solubilized mass

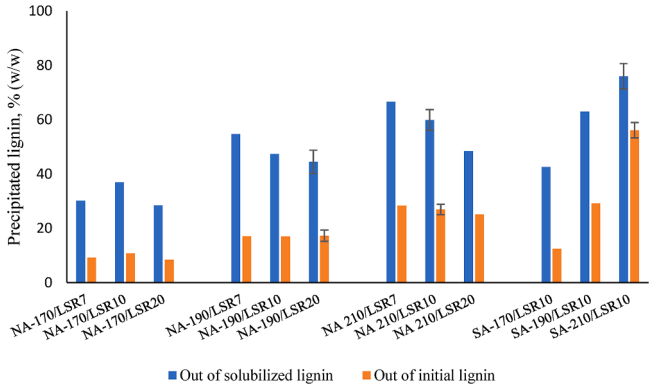

Fig. 1. Yield of regenerated lignin out of precipitated mass (blue columns) and out of initial lignin content (orange columns), % (w/w). NA, non-acidified; SA sulfuric acid-assisted treatment; 170, 190, and 210 indicate treatment temperatures in °C.

decreased with the increase of LSR from 7 to 20.

The observed incomplete regeneration of GVL-solubilized lignin has been reported previously for other materials, such as corn stalk (Wang et al., 2019) and eucalyptus chips (Lê et al., 2016). Lignin precipitation can be enhanced by modulating GVL concentration in the treatment liquor in sequences of water addition, separation of precipitated lignin and further reduction of GVL concentration in successive steps (Wang et al., 2019). Other approaches are inducing biphasic state formation by adding sodium chloride followed by a five-fold addition of deionized water to the lignin-rich GVL phase (Zhou et al., 2018) or combining sodium chloride addition with ultrasonic treatment (Li et al., 2017). In our experiments, a moderate increase of the volume of added water did not help, and we avoided adding larger volumes because of economic reasons. Applying ultrasonic treatment was attempted, but it resulted in only some minor positive effect on recovery of precipitated lignin.

3.4. Characterization of regenerated lignins

3.4.1. Compositional analysis by two-step treatment with sulfuric acid

The compositional analysis showed that lignin content was above 93% (w/w) for all the regenerated samples (Table 3). That indicates that independently of how efficient the solubilization and regeneration processes were, all the regenerated lignins have high purity. The achieved purity is comparable or even higher than that of previous studies on lignin extraction from HL from other biomass sources. Lignin extracted from corn straw HL by alkaline treatment followed by acid precipitation, and sequential redissolution in glycerol-ethanol mixtures reached 84 – 90% (Liu et al., 2018). In another study, 96% purity was achieved after lignin extraction from corn stalk HL by alkaline

Table 3
Results of pyrolysis-GC/MS analysis of regenerated lignins (RL), treatment residues (SR) and non-treated hydrolysis lignin. Lignin content as determined by TSSA analysis is also included. The codification is the same as in Table 1. Means of at least triplicate analyses. Different superscripted uppercase letters denote significant differences at an alpha level of 0.05 according to a Fisher's least significant difference (LSD) test. Like-lettered groups are not significantly different.

Treatment	Temperature (°C)/LSR	Sample	Carbohydrates, % (PAF)	Lignin [a], %(PAF)	Lignin [b], %(w/w)	Δ^{c}_{Lignin}
Non-treated hydrolysis lignin			71.4^{E} (4.2)	21.4^{E} (1.6)	53.5^{D} (1.2)	32.1
NA-GVL	170/7	SR	80.3^{BC} (2.3)	17.2^{F} (1.5)	44.7^{F} (<0.1)	27.5
NA-GVL	170/7	RL	8.3^{G} (1.2)	89.3^{ABC} (0.6)	95.0^{B} (1.4)	5.7
NA-GVL	190/7	SR	76.9^{CD} (4.0)	16.4^{F} (0.5)	44.1^{F} (2.2)	27.7
NA-GVL	190/7	RL	8.4^{G} (1.4)	87.1^{C} (3.1)	95.0^{B} (1.6)	7.9
NA-GVL	210/7	SR	80.1^{BC} (2.0)	16.1^{F} (1.9)	41.6^{G} (0.5)	25.5
NA-GVL	210/7	RL	5.7^{GH} (0.5)	90.6^{AB} (2.5)	96.8^{A} (0.7)	6.2
NA-GVL	210/10	SR	79.5^{BC} (2.9)	15.7^{F} (2.9)	40.0^{HI} (0.5)	24.3
NA-GVL	210/10	RL	6.7^{GH} (0.5)	89.0^{BC} (1.9)	95.5^{AB} (0.4)	6.5
NA-GVL	210/20	SR	75.0^{DE} (6.0)	17.6^{F} (4.2)	36.6^{I} (0.8)	19.0
NA-GVL	210/20	RL	7.3^{GH} (0.9)	90.1^{ABC} (1.8)	96.8^{A} (1.3)	6.7
SA-GVL	170/10	SR	79.6^{BC} (2.9)	17.5^{F} (2.1)	46.3^{E} (1.0)	28.8
SA-GVL	170/10	RL	13.5^{F} (1.1)	81.3^{D} (2.1)	93.1^{C} (1.1)	11.8
SA-GVL	190/10	SR	84.8^{A} (1.7)	12.2^{G} (0.8)	41.1^{GH} (0.1)	28.9
SA-GVL	190/10	RL	5.9^{GH} (0.2)	87.2^{C} (3.2)	93.0^{C} (2.1)	5.8
SA-GVL	210/10	SR	82.6^{AB} (8.7)	9.5^{G} (0.1)	39.3^{I} (1.0)	29.8
SA-GVL	210/10	RL	4.1^{H} (0.3)	92.4^{A} (2.4)	94.5^{BC} (1.4)	2.5

[a] Lignin content determined by Py-GC/MS analysis (PAF, peak area fraction); [b] Lignin content as determined by TSSA analysis (mass fraction); [c] Difference between TSSA lignin and Py-GC/MS lignin.

treatment, followed by acid precipitation, solubilization in a 60:40 GVL/water solution, and successive fractionation by decreasing GVL concentration down to 5% (Wang et al., 2019). Since reaching such a dilution of 80% GVL liquors would require around 15 volumes of water, which appears economically unfavorable, applying that approach was discarded in our study.

3.4.2. Compositional analysis by Py-GC/MS

In order to verify the composition of the regenerated lignins, Py-GC/MS analysis was performed, and the results were compared with those of the TSSA compositional analysis. For regenerated lignins from treatment with NA-GVL, samples from different LSR at a given temperature and from different temperatures at a given LSR were analyzed (Table 3). For the SA-GVL treatment, samples from all experimental conditions were analyzed. Solid resides from the corresponding treatments, as well as non-treated HL, were also included in the analysis. The lignin content resulting from Py-GC/MS analysis ranged between 87.1 and 90.6% for regenerated lignins from NA-GVL treatment (Table 3), and between 81.3 and 92.4% for those from SA-GVL treatment. Between 4.1 and 13.5% of the pyrogram signals were attributed to carbohydrates. For solid residues after treatment, the lignin content ranged from 9.5 % to 17.2%, and the carbohydrate content was above 75%, while for non-treated HL, the lignin-derived signals represented 21.4% and the carbohydrate contribution was 71.4%.

Py-GC/MS lignin values are lower than those of TSSA analysis, while for carbohydrates is the other way around (Table 3). The difference can be attributed to pseudo-lignin, a product of degradation of biomass polysaccharides, mainly hemicelluloses, during thermal processing (Normark et al., 2016). Pseudo-lignin can have been formed during spruce pretreatment prior to HL generation or even during GVL treatment of HL. Pseudo-lignin, which is not soluble in acid, is not detected by TSSA analysis, where the reported Klason lignin includes both real lignin and pseudo-lignin without distinguishing between them. On the other hand, since pseudo-lignin is not composed of phenylpropane units, but consists of carbohydrate-degradation products, Py-GC/MS detects it as carbohydrate-related signals rather than as lignin signals (Wang et al., 2018). Hence, differently to TSSA analysis, Py-GC/MS characterizes pseudo-lignin as carbohydrates. Using the Δ_{Lignin} factor recently introduced by Ilanidis et al. (2021a), Py-GC/MS lignin values are subtracted from the total lignin of the TSSA analysis, which is a practical way to estimate pseudo-lignin content. The Δ_{Lignin} values show that the pseudo-lignin content in HL was 32.1% (Table 3). That high content of pseudo-lignin was predictable considering that previous studies have reported pseudo-lignin formation after steam pretreatment of Norway spruce under conditions covering the range of those used for generating the HL used in this work (Wang et al., 2018). Pseudo-lignin formation after pretreating other feedstocks under comparable conditions has also been reported (Shinde et al., 2018).

For NA-GVL treatments, Δ_{Lignin} values ranged between 5.7 and 7.9 in the regenerated lignins, and for the SA-GVL treatments, they ranged between 2.5 and 11.8 (Table 3). That means that pseudo-lignin contained in HL was partially solubilized by GVL treatment and some of it was precipitated after water addition and was recovered in the regenerated lignin. Anyway, in consistence with the TSSA analysis, the Py-GC/MS results confirm that precipitated lignins after GVL treatment have high lignin content and low content of carbohydrate-derived products.

The regenerated lignin sample with the highest lignin content (92.4%) and with the lowest content of carbohydrates (4.1%) and pseudo-lignin (2.5%) was the one resulting from the SA-GVL treatment at 210 °C (Table 3). Correspondingly, the solid residue of that treatment had the lowest lignin content (9.5%) and the highest content of pseudo-lignin (29.8%). For SA-GVL treatment, increasing the temperature from 170 °C to 210 °C resulted in an increase of the lignin content of regenerated lignin (from 81.3% to the 92.4%), while the Δ_{Lignin} values indicated a clear decrease of pseudo-lignin content from 11.8 to 2.5% as the temperature increased. On the other hand, for NA-GVL treatment, Δ_{Lignin} was not clearly affected by the temperature, but some increase with the LSR increase at 210 °C was evident.

In the treatment solid residues, Δ_{Lignin} values were lower than in HL, and they were not majorly affected by the temperature in any of the treatment approaches (Table 3). However, it is noteworthy that Δ_{Lignin} values in the residues of NA-GVL treatment decreased from 25.5 to 19.0 with the LSR increase at 210 °C.

3.4.3. Molecular weight characterization

To investigate the effects of treatment conditions on the weight-average molecular weight (M_w), number-average molecular weight (M_n), and polydispersity of extracted lignin, HPSEC analysis was conducted. For lignins obtained by NA-GVL treatment, the M_w values ranged from 10 100 to 32 100, while M_n was between 6 100 and 15 000 (Fig. 2). M_w correlated well with reported values for spruce milled wood lignin, which can vary between 11 200 and 29 600 depending on the isolation and purification conditions (Balakshin et al., 2020). No considerable changes were observed in M_w and M_n values by increasing LSR from 7 to 20 at 210 °C. By contrast, increasing the temperature at

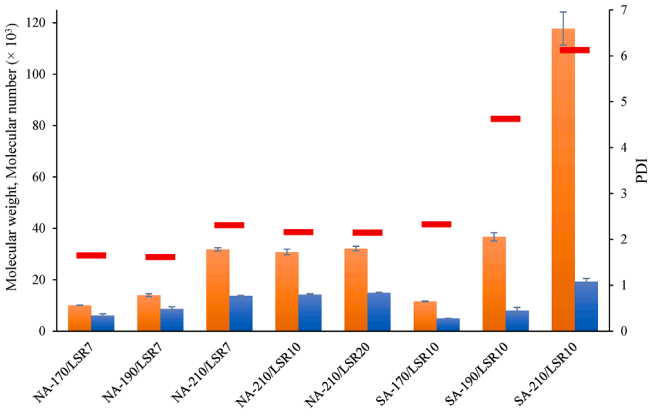

Fig. 2. Weight-average molecular weight (M_W) (orange bars), number-average molecular weight (M_n) (blue bars), and polydispersity index (PDI) (red lines) of regenerated lignins extracted by GVL treatment. The codification on the horizontal axis is the same as in Fig. 1.

LSR 7 led to increase of M_W and M_n. The PDI values, calculated as the M_W/M_n ratio, were between 1.6 and 2.3, and they were affected by the temperature but not by the LSR.

For the lignins from SA-GVL treatment, a clear increase of the M_W and M_n values with the temperature increase was observed. The lignin resulting from SA-GVL treatment at 210 °C resulted in M_W and PDI values of 117 800 and 6.1, respectively. Those values are consistent with previous studies reporting that GVL treatment under severe conditions results in heterogeneous lignins displaying high PDI values (Ahmed et al., 2020). Lignin recondensation under harsh treatment condition could potentially be the reason of the increment of the M_W, and consequently the PDI (Li et al., 2017).

The rather narrow molecular weight distribution, as revealed by the relatively low PDI values, of NA-GVL lignins points towards a homogeneous polymer with favorable features for subsequent downstream processing to value-added applications (Ma et al., 2021). On the other hand, although treatment at higher temperature or after adding acid caused improvement in the yield of regenerated lignin, the high PDI of the resulting product might be a limitation for certain uses. So, the narrow molecular weight distribution of samples extracted by NA-GVL treatment and the broad distribution of those resulting from SA-GVL treatment might anticipate different mechanical properties, and consequently different potential applications, of the lignins depending on the treatment approach (Barana et al., 2016).

3.4.4. CP/MAS ^{13}C NMR analysis

Structural features of HL, selected regenerated lignins and their corresponding treatment residues were investigated using CP/MAS ^{13}C NMR spectroscopy (see supplementary material). The samples selected for the analysis were those from treatments at 210 °C. Regenerated lignins resulted in a strong signal cluster with chemical shift between δ_C 155 and 102 ppm, corresponding to aromatic carbon (Love et al., 1998). That includes peaks at δ_C 155–140 ppm, δ_C 140–124 ppm, and δ_C 124–102 ppm, assigned, respectively, to aromatic C-O, C–C and C–H linkages. The signals in this aromatic region are a typical indication of syringyl (S), guaiacyl (G) and *p*-hydroxyphenyl (H) aromatic units of lignin (An et al., 2015). The spectra of regenerated lignin samples displayed also a very strong and well-defined peak at δ_C 57 ppm, typically assigned to methoxy groups of S or G units of lignin (Casas et al., 2012). As the feedstock used for producing the HL used in this study was spruce, a softwood species, the signals both in the aromatic region and for the methoxy peak can be attributed to G units.

The intensity of all the above-mentioned lignin-related signals was comparable in the spectra of regenerated lignins from both treatment approaches. Some apparent minor differences were related to a variable intensity of the aromatic signals at δ_C 125 ppm (stronger for SA-GVL) and 115 ppm (stronger for NA-GVL).

In the spectra of treatment residues and HL, the relative intensity of the lignin-related peaks (those of the cluster between δ_C 155 and 102 ppm and that at δ_C 56 ppm) was lower than in those of regenerated lignins. Those signals were weaker for the treatment residues than for HL, which is a consequence of lignin removal during treatment. The spectra of the solid residues of the NA- GVL treatment displayed slightly more intense lignin-related signals than those of the residue of the SA-GVL treatment, which is in accordance with the previously discussed lignin solubilization trend (Tables 1 and 2). On the other hand, the peaks in the signal cluster with chemical shift between δ_C 105 and 62 ppm, typically assigned to anhydroglucose carbon atoms in cellulose macromolecules, displayed high intensity in the spectra of treatment residues and HL, whereas they were not detectable in the spectra of regenerated lignins. That includes the C1 peak at δ_C 105 ppm, the C4 peak of crystalline cellulose at δ_C 89, the C4 peak of amorphous cellulose δ_C 84, the C2, C3, and C5 peaks at δ_C 73–76 ppm, and the C6 peaks at δ_C 65 ppm for crystalline cellulose and at δ_C 62 ppm for amorphous cellulose (VanderHart and Atalla, 1984, Normark et al., 2016).

The clear difference between the ^{13}C NMR spectra of regenerated lignin, on one side, and those of solid residues and HL, on the other side, confirms the results of TSSA and Py-GC/MS analyses indicating absence of carbohydrates in the regenerated lignin structure. Comparing the spectra of treatment residues with that of HL confirms the cellulose enrichment happening in the solid material as result of lignin solubilization. Peaks related to cellulose crystallinity, namely at δ_C 89 and 65 ppm, were stronger for treatment residues than for HL, which indicates that cellulose remaining in the solids has higher crystallinity than the initial one. Although that might be affected by removal of hemicelluloses from HL during treatment, a plausible explanation is the preferential removal of amorphous cellulose regions due to their higher susceptibility to acid hydrolysis compared to crystalline cellulose regions. It should also be noted that the peaks associated with cellulose crystallinity were stronger for the solid residue of the NA-GVL treatment than for that of SA-GVL treatment, while for the peak at δ_C 84 ppm, associated with amorphous cellulose, the opposite trend was observed. That points towards higher crystallinity of cellulose contained in the NA-GVL treatment residue compared to that of SA-GVL treatment. This is an issue to be considered for choosing suitable uses of the treatment residue, for instance as either starting point for microcrystalline cellulose or as substrate for new enzymatic saccharification trials.

3.4.5. ^{1}H–^{13}C heteronuclear single quantum coherence (HSQC) NMR analysis

Two-dimensional (2D) ^{1}H–^{13}C HSQC NMR was used to investigate the inter-unit linkages and subunits in regenerated lignins from NA-GVL (Fig. 3A) and SA-GVL (Fig. 3B) treatments at 210 °C. Broad peaks can be observed in the aromatic region (δ_C/δ_H 100–140/6–8 ppm) of the spectra. That includes ^{13}C–^{1}H cross signals corresponding to the C_2-H_2 (G_2), C_5-H_5 (G_5) and C_6-H_6 (G_6) coupling of guaiacyl units at δ_C/δ_H 110.8/6.97, 115.0/6.94 and 118.9/6.81 ppm, respectively (Zeng et al., 2013), which are clearly detectable for both samples. For both lignins, the cross signal at δ_C/δ_H 5.42/87.4 ppm, attributed to the C_α-H_α of phenylcoumaran structures, was stronger than that at δ_C/δ_H 4.75/71.9 ppm, assigned to the C_α-H_α of β-O-4 units. That indicates that in both regenerated lignins, the C–C linkages, for example β-5 of phenylcoumaran, are more important than β-O-4 ether linkages, which were split to a large degree during processing. The β-O-4:β-5 peak ratio was around 0.5 for NA-GVL regenerated lignin, whereas for native softwood lignin, that ratio is much higher and can reach 4 (Chakar and Ragauskas, 2004). This result agrees with existing knowledge on changes undergoing in lignin native structures during extraction. Some of those changes result in new C–C linkages that were not present in native lignin (Talebi Amiri et al., 2019).

For regenerated lignin from SA-GVL treatment, although the peaks

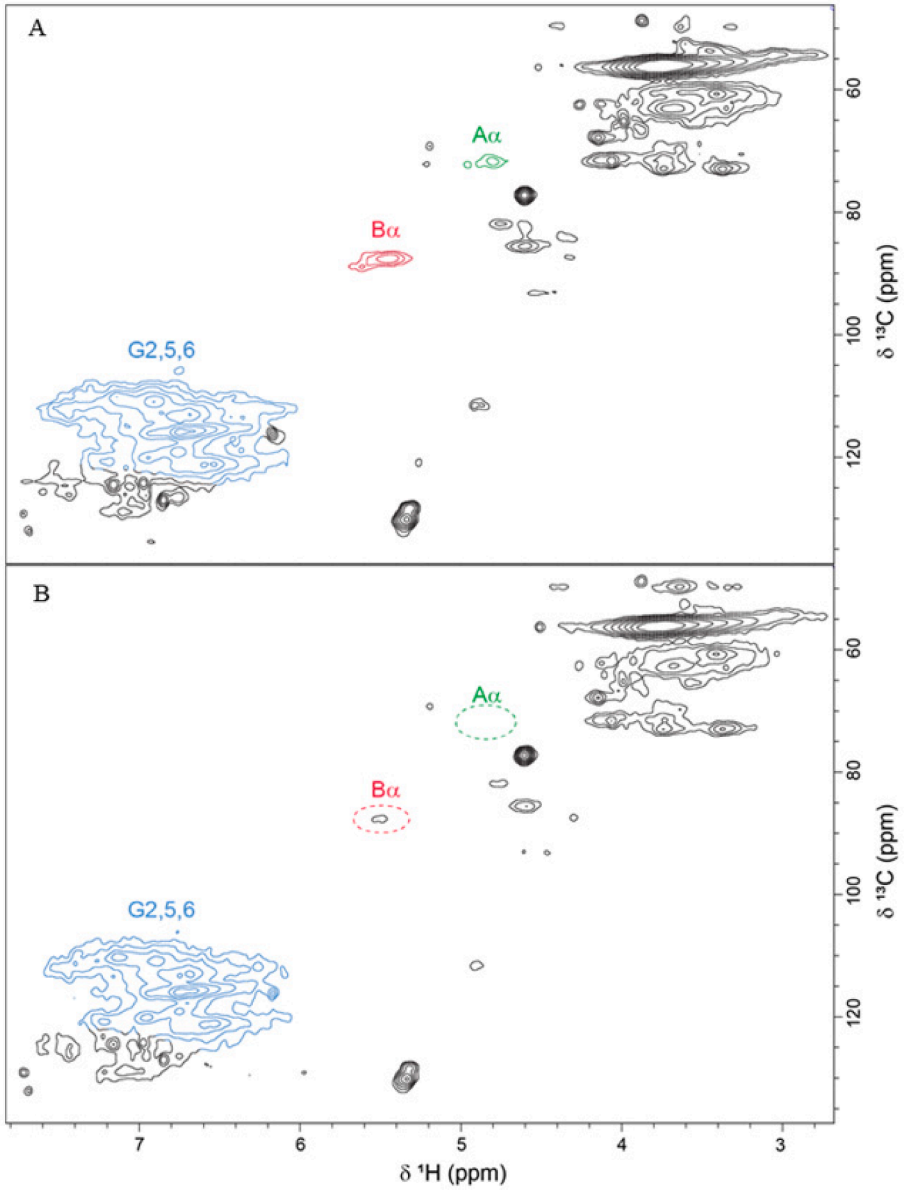

Fig. 3. Two-dimensional ^{1}H–^{13}C HSQC NMR spectra of regenerated lignins from NA-GVL (A) and SA-GVL (B) treatments. Treatment temperature: 210 °C.

were weaker than those of NA-GVL sample, the cross signal of the phenylcoumaran C_{α}-H_{α} was also stronger than that of the β-O-4 unit, which was hardly detectable (Fig. 3B). The high molecular mass of SA-GVL regenerated lignin might have been a possible reason of the lower intensity of the 2D spectral signals (Du et al., 2013).

3.4.6. *FTIR analysis*

The FTIR spectra displayed clear differences between regenerated lignins and HL (see supplementary material). The broad band around 3500 – 3200 cm^{-1}, assigned to stretching vibrations of hydroxyl groups (Jayamani et al., 2020), was remarkably stronger for HL than for regenerated lignins. Although that vibration signal is typical for hydroxyl groups of both polysaccharides and lignin, the stronger intensity for HL can be attributed to cellulose and hemicelluloses contained in the starting material (Table 1). That assumption is confirmed also by the position and shape of the signal, which for HL was more intense towards 3200 cm^{-1}, as typical for cellulose (Kondo, 1997), while for regenerated lignins it was stronger towards 3500 cm^{-1}, as typical for lignin (Rashid et al., 2016). A broad band ranging from around 2900 – 2750 cm^{-1}, attributed to the C–H stretching in methyl and methylene groups of cellulose (Faix, 1992), is observed in the HL spectrum. For regenerated lignins, instead, an intense peak was observed at 2929 cm^{-1}, as typical for lignin C–H stretching, and a weaker but clear signal was detectable at 2800 cm^{-1}, which has previously been observed in lignin (Rashid et al., 2016). The intensity of lignin-related signals around 1595 cm^{-1} (C = C stretching) (Jayamani et al., 2020), 1510 cm^{-1} (aromatic ring stretch), 1460 cm^{-1} (C–H deformation in $–CH_3$ and $–CH_2$), 1423 cm^{-1} (aromatic skeletal vibrations), 1268 cm^{-1} (G ring plus C = O stretch), 1228 cm^{-1} (C–C plus C-O plus C = O stretch), and 1141 cm^{-1} (aromatic C–H in-plane deformation) (Faix, 1992) is considerably stronger in the spectra of regenerated lignins than in that of HL. On the other hand, the cellulose-related peaks at 1035, 1058 and 1110 cm^{-1}, assigned to C–C, C–H and C–OH stretching and deformation vibrations, display higher intensity in the spectrum of HL.

The FTIR spectra of regenerated lignins from both treatment approaches displayed similar characteristics. One of the few minor detectable differences was the signal at 1760 cm^{-1}, visible as a clear peak for the SA-GVL sample but rather as a shoulder for the NA-GVL one. Signals in the 1700 – 1780 cm^{-1} region are typically assigned to C = O stretching vibration of different carbonylic compounds, with those of

esters being around 1740 – 1760 cm^{-1}, and can be attributed to acetyl groups of hemicelluloses (Wang et al., 2018). Since no hemicelluloses were found in the sample, the peak might be related to pseudo-lignin.

4. Conclusion

Treatment with γ-valerolactone was proven to be a suitable method for recovering purified lignin from hydrolysis lignin of steam-pretreated spruce. Assisting the treatment with a low addition of sulfuric acid enhanced the extraction efficiency. The characterization of regenerated lignins from different treatment conditions revealed no major differences apart from the molecular weight distribution, which was broader for samples from sulfuric acid-assisted GVL treatment compared with those from the treatment with non-acidified GVL/water. The difference in molecular weight distribution might result in different mechanical properties of lignin-based materials, and consequently different potential applications for regenerated lignins depending on the treatment approach.

CRediT authorship contribution statement

Forough Momayez: Conceptualization, Formal analysis, Investigation, Methodology, Validation, Visualization, Writing – original draft. **Mattias Hedenström:** Formal analysis, Investigation, Visualization, Writing – review & editing. **Stefan Stagge:** Formal analysis, Methodology, Validation. **Leif J. Jönsson:** Conceptualization, Funding acquisition, Methodology, Project administration, Resources, Writing – review & editing. **Carlos Martín:** Conceptualization, Funding acquisition, Methodology, Project administration, Resources, Supervision, Writing – review & editing.

Declaration of Competing Interest

The authors declare that they have no known competing financial interests or personal relationships that could have appeared to influence the work reported in this paper.

Data availability

Data will be made available on request.

Acknowledgement

The technical platforms and core facilities at the Chemical Biological Center of Umeå University and of the Swedish University of Agricultural Sciences are acknowledged for the support provided with analytical techniques. András Gorzsás (Vibrational Spectroscopy Core Facility) and Junko Takahashi-Schmidt and Ola Sundman (Biopolymer Analytical Platform) are expressly thanked. Special thanks to Pooja Dixit and Madhavi Latha Gandla for all support. Financial support provided by the Kempe Foundations (SMK-1969.6), the Swedish Energy Agency (49699-1), Bio4Energy (www.bio4energy.se) and Sparebankstiftelsen Hedmark (https://sparebankstiftelsenhedmark.no) is gratefully acknowledged.

Appendix

CP/MAS ^{13}C NMR spectra of regenerated lignins and solid residues, as well as FTIR spectra of regenerated lignins and hydrolysis lignin can be found as E-supplementary data in the online version of the paper.

References

Ahmed, M.A., Lee, J.H., Raja, A.A., Choi, J.W., 2020. Effects of gamma-valerolactone assisted fractionation of ball-milled pine wood on lignin extraction and its characterization as well as its corresponding cellulose digestion. Appl. Sci. 10, 1599.
Alonso, D.M., Wettstein, S.G., Dumesic, J.A., 2013. Gamma-valerolactone, a sustainable platform molecule derived from lignocellulosic biomass. Green Chem. 15, 584–595.
An, Y.-X., Li, N., Wu, H., Lou, W.-Y., Zong, M.-H., 2015. Changes in the structure and the thermal properties of kraft lignin during its dissolution in cholinium ionic liquids. ACS Sustain. Chem. Eng. 3, 2951–2958.
Ashokkumar, V., Venkatkarthick, R., Jayashree, S., et al., 2022. Recent advances in lignocellulosic biomass for biofuels and value-added bioproducts - a critical review. Bioresour. Technol. 344, 126195.
Balakshin, M., Capanema, E.A., Zhu, X., et al., 2020. Correction: Spruce milled wood lignin: linear, branched or cross-linked? Green Chem. 22, 8046-8046.
Barana, D., Ali, S., Salanti, A., et al., 2016. Influence of lignin features on thermal stability and mechanical properties of natural rubber compounds. ACS Sustain. Chem. Eng. 4, 5258–5267.
Casas, A., Oliet, M., Alonso, M.V., Rodríguez, F., 2012. Dissolution of *Pinus radiata* and *Eucalyptus globulus* woods in ionic liquids under microwave radiation: Lignin regeneration and characterization. Sep. Purif. Technol. 97, 115–122.
Chakar, F.S., Ragauskas, A.J., 2004. Review of current and future softwood kraft lignin process chemistry. Ind. Crops Prod. 20, 131–141.
Du, X., Gellerstedt, G., Li, J., 2013. Universal fractionation of lignin–carbohydrate complexes (LCCs) from lignocellulosic biomass: an example using spruce wood. Plant J. 74, 328–338.
Evstigneyev, E.I., Yuzikhin, O.S., Gurinov, A.A., et al., 2016. Study of structure of industrial acid hydrolysis lignin, oxidized in the H_2O_2-H_2SO_4 system. J. Wood Chem. Technol. 36, 259–269.
Faix, O., 1992. Fourier transform infrared spectroscopy. In: Lin, S.Y., Dence, C.W. (Eds.), in: methods in lignin chemistry. Springer, Berlin Heidelberg. Berlin, Heidelberg, pp. 83–109.
Fengel, D., Wegener, G., 1989. Wood—chemistry, ultrastructure, reactions. J. Polym. Sci. Polym. Lett. Ed. 23, 601–602.
Galbe, M., Wallberg, O., 2019. Pretreatment for biorefineries: a review of common methods for efficient utilisation of lignocellulosic materials. Biotechnol. Biofuels 12, 294.
Gerber, L., Eliasson, M., Trygg, J., et al., 2012. Multivariate curve resolution provides a high-throughput data processing pipeline for pyrolysis-gas chromatography/mass spectrometry. J. Anal. Appl. Pyrolysis 95, 95–100.
Ilanidis, D., Stagge, S., Jönsson, L.J., Martín, C., 2021a. Effects of operational conditions on auto-catalyzed and sulfuric-acid-catalyzed hydrothermal pretreatment of sugarcane bagasse at different severity factor. Ind. Crops Prod. 159, 113077.
Ilanidis, D., Wu, G., Stagge, S., Martín, C., Jönsson, L.J., 2021b. Effects of redox environment on hydrothermal pretreatment of lignocellulosic biomass under acidic conditions. Bioresour. Technol. 319, 124211.
Jayamani, E., Loong, T.G., Bakri, M.K.B., 2020. Comparative study of Fourier transform infrared spectroscopy (FTIR) analysis of natural fibres treated with chemical, physical and biological methods. Polym. Bull. 77, 1605–1629.
Jia, L., Qin, Y., Wang, J., Zhang, J., 2020. Lignin extracted by γ-valerolactone/water from corn stover improves cellulose enzymatic hydrolysis. Bioresour. Technol. 302, 122901.
Jönsson, L.J., Martín, C., 2016. Pretreatment of lignocellulose: Formation of inhibitory by-products and strategies for minimizing their effects. Bioresour. Technol. 199, 103–112.
Kondo, T., 1997. The assignment of IR absorption bands due to free hydroxyl groups in cellulose. Cellulose 4, 281–292.
Lê, H.Q., Ma, Y., Borrega, M., Sixta, H., 2016. Wood biorefinery based on γ-valerolactone/water fractionation. Green Chem. 18, 5466–5476.
Li, S.-X., Li, M.-F., Yu, P., et al., 2017. Valorization of bamboo by γ-valerolactone/acid/water to produce digestible cellulose, degraded sugars and lignin. Bioresour. Technol. 230, 90–96.
Liu, C., Si, C., Wang, G., et al., 2018. A novel and efficient process for lignin fractionation in biomass-derived glycerol-ethanol solvent system. Ind. Crops Prod. 111, 201–211.
Love, G.D., Snape, C.E., Jarvis, M.C., 1998. Comparison of the leaf and stem cell-wall components in barley straw by solid-state ^{13}C NMR. Phytochemistry 49 (5), 1191–1194.
Lowe, R.J., Drummond, P., 2022. Solar, wind and logistic substitution in global energy supply to 2050 – Barriers and implications. Renew. Sust. Energ. Rev. 153, 111720.
Ma, C.-Y., Peng, X.-P., Sun, S., et al., 2021. Short-time deep eutectic solvents pretreatment enhanced production of fermentable sugars and tailored lignin nanoparticles from abaca. Int. J. Biol. Macromol. 192, 417–425.
Martín, C., Dixit, P., Momayez, F., Jönsson, L.J., 2022. Hydrothermal pretreatment of lignocellulosic feedstocks to facilitate biochemical conversion. Front. Bioeng. Biotechnol. 10, 846592.
Normark, M., Pommer, L., Gräsvik, J., Hedenström, M., Gorzsás, A., Winestrand, S., Jönsson, L.J., 2016. Biochemical conversion of torrefied Norway spruce after pretreatment with acid or ionic liquid. BioEnergy Res. 9, 355–368.
Oliva-Taravilla, A., Carrasco, C., Jönsson, L.J., Martín, C., 2020. Effects of biosurfactants on enzymatic saccharification and fermentation of pretreated softwood. Molecules 25, 3559.
Ragauskas, A.J., Beckham, G.T., Biddy, M.J., et al., 2014. Lignin valorization: improving lignin processing in the biorefinery. Science 344, 1246843.
Ralph, J., Lapierre, C., Boerjan, W., 2019. Lignin structure and its engineering. Curr. Opin. Biotechnol. 56, 240–249.
Rashid, T., Kait, C.F., Murugesan, T., 2016. A "Fourier Transformed infrared" compound study of lignin recovered from a formic acid process. Procedia Eng. 148, 1312–1319.
Shinde, S.D., Meng, X., Kumar, R., Ragauskas, A.J., 2018. Recent advances in understanding the pseudo-lignin formation in a lignocellulosic biorefinery. Green Chem. 20, 2192–2205.
Shuai, L., Questell-Santiago, Y.M., Luterbacher, J.S., 2016. A mild biomass pretreatment using γ-valerolactone for concentrated sugar production. Green Chem. 18, 937–943.

Singh, N., Singhania, R.R., Nigam, P.S., et al., 2022. Global status of lignocellulosic biorefinery: challenges and perspectives. Bioresour. Technol. 344, Part B, 126415.
Sluiter, A., Hames, B., Ruiz, R., et al., 2008. Determination of structural carbohydrates and lignin in biomass. Lab. Anal. Proc. 1617, 1–16.
Talebi Amiri, M., Bertella, S., Questell-Santiago, Y.M., Luterbacher, J.S., 2019. Establishing lignin structure-upgradeability relationships using quantitative ^{1}H–^{13}C HSQC-NMR spectroscopy. Chem. Sci. 10, 8135–8142.
VanderHart, D.L., Atalla, R.H., 1984. Studies of microstructure in native celluloses using solid-state ^{13}C NMR. Macromolecules 17, 1465–1472.
Várnai, A., Siika-aho, M., Viikari, L., 2010. Restriction of the enzymatic hydrolysis of steam-pretreated spruce by lignin and hemicellulose. Enzyme Microb. Technol. 46, 185–193.
Wang, G., Liu, X., Yang, B., et al., 2019. Using green γ-valerolactone/water solvent to decrease lignin heterogeneity by gradient precipitation. ACS Sustain. Chem. Eng. 7, 10112.
Wang, Z., Wu, G., Jönsson, L.J., 2018. Effects of impregnation of softwood with sulfuric acid and sulfur dioxide on chemical and physical characteristics, enzymatic digestibility, and fermentability. Bioresour. Technol. 247, 200–208.
Weiqi, W., Shubin, W., Liguo, L., 2013. Combination of liquid hot water pretreatment and wet disk milling to improve the efficiency of the enzymatic hydrolysis of eucalyptus. Bioresour. Technol. 128, 725–730.
Xu, R., Du, H., Wang, H., et al., 2021. Valorization of enzymatic hydrolysis residues from corncob into lignin-containing cellulose nanofibrils and lignin nanoparticles. Front. Bioeng. Biotechnol. 9.
Xue, Z., Zhao, X., Sun, R.-C., Mu, T., 2016. Biomass-derived γ-valerolactone-based solvent systems for highly efficient dissolution of various lignins: Dissolution behavior and mechanism study. ACS Sustain. Chem. Eng. 4, 3864–3870.
Yin, X., Wei, L., Pan, X., et al., 2021. The pretreatment of lignocelluloses with green solvent as biorefinery preprocess: a minor review. Front. Plant Sci. 12.
Zeng, J., Helms, G.L., Gao, X., Chen, S., 2013. Quantification of wheat straw lignin structure by comprehensive NMR analysis. J. Agric. Food. Chem. 61, 10848–10857.
Zhou, X., Ding, D., You, T., et al., 2018. Synergetic dissolution of branched xylan and lignin opens the way for enzymatic hydrolysis of poplar cell wall. J. Agric. Food. Chem. 66, 3449.